


# Detailed Kinetic Model for the Reaction of Ethene to Propene on Ni/AlMCM-41

Matthias Felischak<sup>1,\*</sup>, Tanya Wolff<sup>2</sup>, Leo Alvarado Perea<sup>3</sup>, Andreas Seidel-Morgenstern<sup>1,2</sup>, and Christof Hamel<sup>1,4</sup>

DOI: 10.1002/cite.201900139

 This is an open access article under the terms of the Creative Commons Attribution-NonCommercial-NoDerivs License, which permits use and distribution in any medium, provided the original work is properly cited, the use is non-commercial and no modifications or adaptations are made.



Supporting Information  
available online

The Ni/AlMCM-41 was prepared and applied as the catalyst for the direct conversion of ethene to propene. Based on the results of the broad experimental study, two reaction networks were compared, one consisting of dimerization, isomerization and metathesis and a modified network suggesting the cracking of long-chain olefins. To correlate the experimentally obtained data, the classical Langmuir-Hinshelwood-Hougen-Watson model was applied for both reaction networks. The second network involving catalytic cracking offers a satisfying prediction of the observed product distributions.

**Keywords:** Parameter estimation, Reaction kinetics, Reactor and kinetic modeling

*Received:* September 13, 2019; *revised:* February 12, 2020; *accepted:* February 27, 2020

## 1 Introduction

Propene has become one of the central building blocks for the petrochemical industry [1]. It is mainly used for the production of the highly demanded polypropylene and propene oxide. The steadily growing demand cannot be easily met by the current production technologies [1], like steam cracking. Therefore, new efficient on-demand technologies are required. The direct conversion of ethene to propene (ETP) [2, 3] is an attractive possibility, exploiting the availability of ethene.

Significant research was dedicated to developing suitable catalytic systems. Taoufik et al. have reported the direct transformation of ethene into propene over a tungsten hydride supported on alumina [4]. The conversion was approx. 10 % after 10 h on stream. Oikawa et al. [5] and Lin et al. [6] presented silica aluminophosphate microporous molecular sieves, e.g., SAPO-34 (small-pore molecular sieves-34) and H-ZSM-5 (Zeolite Socony Mobil-5) zeolites, as highly active catalysts for the ETP reaction, but also faced severe deactivation with time on stream. Iwamoto et al. [3, 7] investigated nickel-doped MCM-41 (Mobil Composition of Matter No. 41) and found it to be active for the ETP reaction. Lehmann et al. [8, 9] and Alvarado Perea et al. [2] studied the characteristics of Ni/MCM-41 and its aluminized counterpart Ni/AlMCM-41. To design and optimize the reaction system, a quantitative description of the underlying reaction mechanisms and kinetics is necessary. The widely accepted mechanism proposed by Iwamoto et al. [3] consists of dimerization, isomerization and metathesis reaction steps (see Fig. 1).

Initially, ethene is dimerized to 1-butene by the nickel ion of the catalyst, followed by the isomerization of 1-butene to *cis/trans*-butene catalyzed by the acidic sites. Finally, a metathesis step of the generated 2-butene and unconverted ethene results in propene. It is supposed that nickel initiates the metathesis step. This catalytic cycle has been discussed in more detail in, e.g., [2, 10, 11]. The relatively simple network postulated does not consider the formation of essential by-products and their influence on the course of the reactions. Additionally, it neglects that nickel is not a typical active metal for metathesis reactions. Therefore, a more detailed reaction network is desirable, considering the relevant side reactions and the ongoing mechanism as the focus of this present contribution.

<sup>1</sup>Matthias Felischak, Prof. Dr.-Ing Andreas Seidel-Morgenstern, Prof. Dr.-Ing Christof Hamel  
Matthias.felischak@ovgu.de

Otto von Guericke University, Institute of Process Engineering, Universitätsplatz 2, 39106 Magdeburg, Germany.

<sup>2</sup>Dr. Tanya Wolff, Prof. Dr.-Ing Andreas Seidel-Morgenstern  
Max Planck Institute for Dynamics of Complex Technical Systems, Sandtorstraße 1, 39106 Magdeburg, Germany.

<sup>3</sup>Dr. Leo Alvarado Perea  
Universidad Autónoma de Zacatecas, Jardín Juárez 147, 98000 Zacatecas, Mexico.

<sup>4</sup>Prof. Dr.-Ing Christof Hamel  
Anhalt University of Applied Sciences, Bernburger Straße 55, 06366 Köthen, Germany.

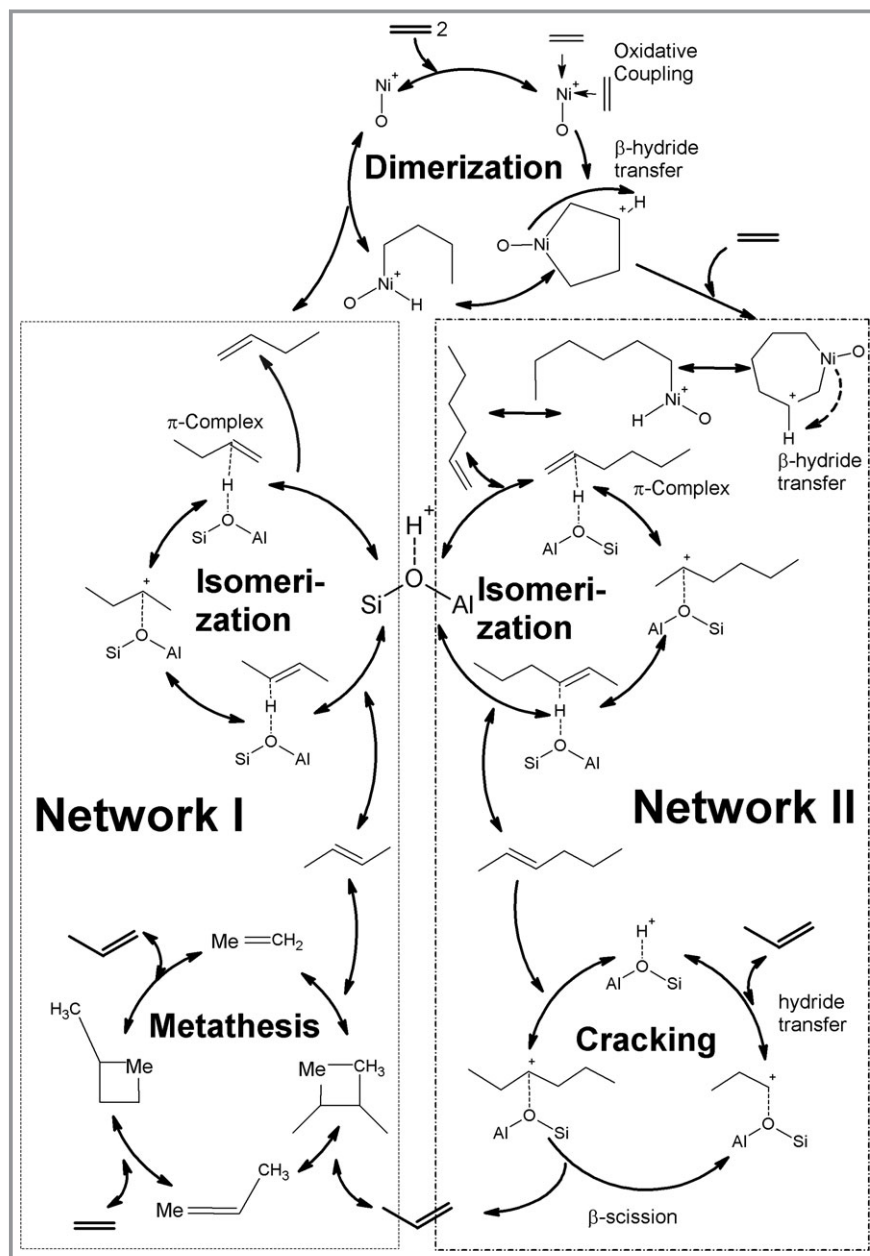


**Figure 1.** Catalytic reaction networks based on dimerization, isomerization combined with metathesis for network I, proposed by Iwamoto, and cracking for the modified network II, proposed in a previous contribution [24].

Many research groups investigated the transformation of hydrocarbons to light olefins for various reaction types. Perez-Uriarte [12] used HZSM-5 for the conversion of dimethyl ether (DME) to olefins. The ZSM-5 was also applied by Beirnaert [13] and Aretin [14] for the cracking of hexene, Epelde [15] for the transformation of 1-butene and Gayubo [16] for ethanol conversion to olefins. Another compelling catalyst is SAPO-34 that was used by Mousavi [17] for the methanol-to-olefin process and by Zhou [18] for the reaction of light alkenes. The methanol-to-olefin

process is an exciting alternative to the well-known feedstock. Therefore, van Speybroeck [19] derived principle kinetics for applied zeolites. Another approach, by Pinto et al. [20], is the application of alkanes, like hexane and heptane. The metathesis reaction as one of the most important organic reactions of the last century was kinetically investigated by, e.g., Lwin [21] and Kapteijn [22]. Buluchevski [23] applied PdO-Re<sub>2</sub>O<sub>7</sub>-B<sub>2</sub>O<sub>3</sub>-Al<sub>2</sub>O<sub>3</sub> for the liquid phase reaction of ethene to propene.

Recently, it was assumed that catalytic cracking of long-chain olefins to the desired short-chain olefins occurs [24]. The applied aluminized MCM-41 belongs to a class of supports catalyzing this type of reaction [25]. Several investigations exploiting MCM [26,27] and ZSM [28–30] have been performed. The cracking mechanism is considered to be based on the protolytic scission of the double-bonded atoms, resulting in separate olefinic molecules [31,32]. In comparison to the cracking mechanism described, the metathesis is thoroughly investigated [33–35]. Both catalytic cycles are shown and discussed in Fig. 1. These cycles provide a suitable basis for the derivation of similar kinetic rate laws. So far, no reliable kinetic model equations were provided for predicting the direct conversion of ethene on Ni/AlMCM-41 (Si/Al = 60) to propene.

The focus of this work will be the analysis and parametrization of two detailed kinetic models. The first model is based on the reaction network suggested by Iwamoto, including metathesis. The second model is

based on the modified network, including cracking reactions. In both cases, the Langmuir-Hinshelwood-Hougen-Watson (LH) rate expressions are applied for the kinetic description of the system [36,37]. The approach considers the elementary steps of the two catalytic cycles postulated [38–41].

## 2 Experimental Procedure

### 2.1 Preparation of Support and Catalyst

The (Al)MCM-41 support was prepared by the method described by Alvarado-Perea et al. [10]. The precursor mixture had a molar composition of 1 SiO<sub>2</sub>/0.35 CTABr/0.31 TBAOH/0.000–0.2 NaAlO<sub>2</sub>/55 H<sub>2</sub>O and was stirred for 15 min. Sodium aluminate (NaAlO<sub>2</sub>/Al<sub>2</sub>O<sub>3</sub> 50–56 % and Na<sub>2</sub>O 40–45 %) was used as the aluminum source, with its amount being adjusted for generating a Si/Al ratio of 60. Subsequently, the mixture was filled into a PTFE bottle and aged 48 h at 100 °C in an oven. The resulting white solid was recovered by vacuum filtration and washed with deionized water. The produced powder was dried and calcinated, as reported by Alvarado-Perea et al. [2], to carry out the corresponding characterization.

The Ni/AlMCM-41 catalyst was prepared using the template ion-exchange method. Nickel nitrate (Merck, Ni<sub>2</sub>(NO<sub>3</sub>)<sub>2</sub>·6H<sub>2</sub>O ≥ 99.0 %) was used as a Ni precursor. The resulting mixture was thermally treated in a PTFE bottle in a muffle furnace. The light green solid was subsequently recovered through vacuum filtration, washed and dried. The final product was calcinated at 600 °C for 6 h in air. The characterization of Ni/AlMCM-41 was done using XRD, N<sub>2</sub> physisorption, TEM, AAS, TPR, TPO, Si CP-MAS NMR and Al MAS NMR as reported in [2].

### 2.2 Catalyst Testing

A comprehensive evaluation of the kinetics of the catalyst was carried out in a fixed-bed laboratory reactor equipped with an oven. The applied quartz tube had an inner diameter of 0.6 cm. All experiments were performed at atmospheric pressure, with the same amount of 0.5 g of catalyst, causing a bed length of 11.8 cm. The feed consisted of ethene (Linde, 99.9 %) and nitrogen (Linde, 99.9993 %). Different sets of experiments were performed. The following conditions were varied during the extensive experimental study: space velocity (weight of catalyst/flowrate, *W/F*) in the range of 250–750 kg<sub>Cat</sub>s m<sup>-3</sup> and molar fraction of ethene in the feed between 2.5 and 25 %, with the rest being nitrogen. To quantify the corresponding dependence, the temperature was varied between 50 and 350 °C in increments of 25 °C. The analysis of the composition of the reactant inlet stream and the reaction products was carried out using a gas chromatography (Agilent 6890 GC/TCD with a 5973 MSD) equipped with a 30-m HP-Plot Q column (Agilent Technologies).

After each experimental run, the catalyst bed was regenerated to retrieve the catalyst's initial activity and to have comparable conditions. For this, the fixed bed was heated up to 500 °C under nitrogen. When the desired temperature was reached, compressed air was added to the feed stream and the conditions were kept constant for 1 h. The

airstream was adjusted to the oxygen concentration for guaranteeing the oxidation of carbonaceous residue. After this oxidation procedure, the reactor was cooled under nitrogen down to 50 °C. Applying this procedure, the catalyst revealed an unchanged behavior and in subsequently carried out reference runs a good reproducibility was obvious. The full set of experiments performed consisted of *N<sub>ex</sub>* = 120 runs.

## 3 Postulation of Reaction Networks

A reaction network has to be postulated to estimate kinetic parameters. In this contribution, the well-established network suggested by Iwamoto [3] (network I) and a modified network, including cracking reactions (network II) as intensively discussed in the introduction (Fig. 1) were applied.

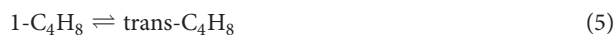
### 3.1 Network Proposed by Iwamoto (Network I)

The set of reactions resulting from the mechanism of the ETP reaction proposed by Iwamoto [3] is presented in Eqs. (1)–(16) as network I. The network consists of *L*<sub>1</sub> = 7 species involved in *J*<sub>1</sub> = 16 elementary reactions, utilizing the assumed catalytic cycles in Fig. 1. It includes the oligomerization of ethene (Eqs. (1) and (2)), another hexene formation reaction (Eq. (3)), isomerization reactions (Eqs. (4)–(6)) and metathesis reactions (Eqs. (7)–(16)) in contrast to network II.

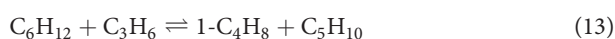
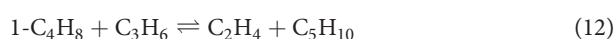
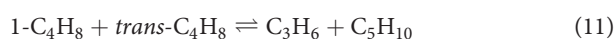
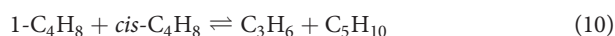
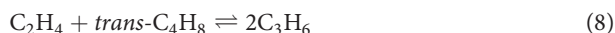
#### *Di-/Oligomerization*

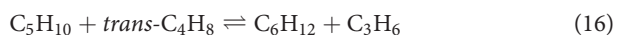
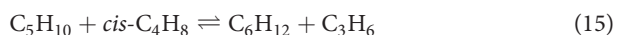
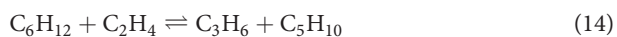


#### *Isomerization*



#### *Metathesis (Characteristic for Network I)*





Such detailed reaction networks correlate with a high number of kinetic parameters. Nevertheless, they are necessary for detailed mechanistic description, accounting for all occurring effects. Especially gas-phase reactions [42, 43] and complex reactions, like pyrolysis [44, 45], result in excessive numbers of parameters.

### 3.2 Modified Network Including Cracking (Network II)

Based on the product analysis performed and the obtained experimental perceptions, the mentioned network I was found to be incapable of accounting for all phenomena observed [24]. Formation of larger olefins, such as pentenes and hexenes, can be explained by the metathesis of specific intermediates and oligomerization of ethene, following a pseudo-Wittig mechanism [46]. However, this is not typically observed. Especially, because retro-metathesis reactions with propene as feed do not produce the assumed equimolar ratio of ethene and 2-butene. Instead, mainly, hexenes are detected. The appearance of saturated hydrocarbons, like ethane, and the generation of coke species cannot be explained sufficiently [47]. Although chain length growth is an application of metathesis. Upon network analysis, a modified reaction mechanism, including cracking rather than metathesis, illustrated in Fig. 1, results in a new set of reaction equations. According to the literature [48–52], active nickel sites catalyze the oligomerization of ethene. The main products of this step are butenes. This mechanism proceeds via the oxidative coupling of ethene [53, 54]. However, ethene could be further oligomerized to hexene. Besides, the butenes may dimerize as well or the coupling of ethene with butenes (Eq. (3)) can occur. Resulting in longer chain olefins, e.g. hexene or octene, which can isomerize to the thermodynamically favored internal olefin, via  $\pi$ -allylic carbanion using acidic sites of the catalyst [55]. The mechanism proposed in this contribution involves a conjunct polymerization up to hexene [11, 56], with subsequent cracking [31, 32, 57, 58]. The wide range of possible molecules can interact with the acidic sites, creating a complex network of cracking reactions. The described pathway explains the product spectrum observed in our investigations and the reaction towards propene.

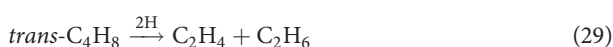
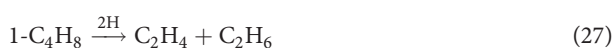
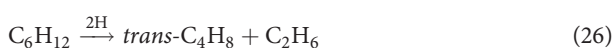
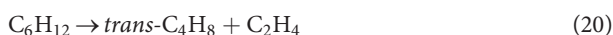
The cracking reaction proceeds via monomolecular protolytic cracking by  $\beta$ -scission of the longer chain olefins, as shown in Fig. 1. Further oligomerization, aromatization and deprotonation may occur as side reactions. This occurring effect is an explanation for the generation of alkanes and the severe deactivation, due to the production of coke and

the following blocking of active sites obtained during experiments. Thus, a reaction network, including catalytic cracking of formed 3-hexene, which predominantly results in the desired product propene, is suggested. With this extended and more complex reaction mechanism (network II) the total number of feasible reactions increases to  $J_{II} = 24$ , when it is limited to the highest analyzable olefin hexene. Due to the inclusion of ethane, the number of species considered is now  $L_{II} = 8$ , in contrast to network I. To reduce the complexity all isomers of pentene are lumped together as  $\text{C}_5\text{H}_{10}$  and  $\text{C}_6\text{H}_{12}$ .

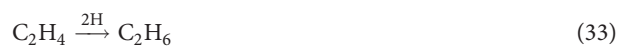
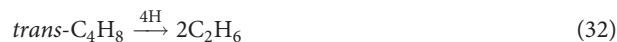
The set of reaction equations quantified in the modified network II consists of Eqs. (1)–(6) as part of network I and maintained here. The metathesis reactions (Eqs. (7)–(16)) considered in network I are replaced by Eqs. (17)–(34) corresponding to the cracking mechanism (network II) described above.

Hydrogen is not explicitly considered in this network. Though, from the literature [47] it is clear that the high-temperature hydrocarbon reaction does present the possibility to form polyenes or cyclic molecules. Thus, it is possible that hydrogen is released and immediately interacts with occurring unsaturated hydrocarbons to form alkanes. This conclusion is supported by the observation in previous publications where the content of saturated hydrocarbon from olefin feedstock increased with increasing temperature and time on stream, while the coking is enhanced. Coke is believed to be of long-chain olefinic, polyenic and cyclic nature.

#### Cracking (characteristic for network II)







In our investigation, the different reaction networks introduced above (network I, Eqs. (1)–(16), and the modified network II, Eqs. (1)–(6) and Eqs. (17)–(34)) are evaluated and compared using the extensive set of experimental data acquired. The kinetic model applied was for the LH assumption.

## 4 Generation of Kinetic Expressions

The most investigations for the direct conversion of ethene to propene were dedicated to the preparation of catalysts and their characterization concerning activity. Limited attention was devoted to the quantitative description of kinetics [16, 19, 20, 59]. These are required for further process optimization concerning the reactor setup, feeding strategies and optimal process control. Typically, only simple reaction mechanisms such as power laws have been used in previous publications [14, 60, 61]. In the present contribution, a detailed kinetic model has been applied and evaluated to the mentioned reaction networks based on the preposition by Iwamoto (network I) and the modified, including cracking (network II).

### 4.1 Langmuir-Hinshelwood-Hougen-Watson Kinetics (LH)

A quantifying rate law of heterogeneously catalyzed reactions is based on LH models [37]. The approach exploits the Langmuir adsorption isotherm model. Applying the generally known procedure for deriving LH rate expressions for the assumed surface reactions: dimerization, isomerization, metathesis and cracking can be treated in a straightforward manner [62]. It is assumed that all the molecules, reactants and products in each reaction can adsorb onto the catalyst surface. For that reason, applying the LH kinetics for the catalytic reaction steps, shown in Fig. 1, the following general rate equation is obtained for the dimerization reaction (Eq. (1)) considered as an irreversible reaction:

$$\text{Dimerization}$$

$$r_{\text{Dim}}^{\text{LH}} = \frac{k_{\text{Dim}}^{\text{LH}} K_{\text{C}_2\text{H}_4, \text{LH}}^2 P_{\text{C}_2\text{H}_4}^2}{1 + K_{\text{C}_2\text{H}_4, \text{LH}} P_{\text{C}_2\text{H}_4} + K_{1-\text{C}_4\text{H}_8, \text{LH}} P_{1-\text{C}_4\text{H}_8}^2} \quad (35)$$

$K_i$  values represent the component-specific adsorption equilibrium constants, in Eq. (35)  $K_{\text{C}_2\text{H}_4}$  for ethene, and  $K_{1-\text{C}_4\text{H}_8}$  for 1-butene.

In accordance to this procedure, the following equations can be derived for the rates of the isomerization (Eq. (5)), metathesis (Eq. (8)), which correlates to network I, and cracking (Eq. (17)), which is the subsequent step following dimerization and isomerization in network II. With this, based on the results of preliminary research [33–35, 55, 63–65], the isomerization and the metathesis reactions are considered to be reversible reactions, which is implemented as the backward reaction in the kinetic approaches.

#### Isomerization

$$r_{\text{Iso}}^{\text{LH}} = \frac{k_{\text{Iso}}^{\text{LH}} K_{1-\text{C}_4\text{H}_8, \text{LH}} P_{1-\text{C}_4\text{H}_8} - \frac{1}{K_{\text{P, Iso}}} K_{\text{trans-C}_4\text{H}_8, \text{LH}} P_{\text{trans-C}_4\text{H}_8}}{1 + K_{1-\text{C}_4\text{H}_8, \text{LH}} P_{1-\text{C}_4\text{H}_8} + K_{\text{trans-C}_4\text{H}_8, \text{LH}} P_{\text{trans-C}_4\text{H}_8}} \quad (36)$$

#### Metathesis (characteristic of network II) Eq. (38)

$$r_{\text{Met}}^{\text{LH}} = \frac{k_{\text{Met}}^{\text{LH}} K_{\text{C}_2\text{H}_4, \text{LH}} P_{\text{C}_2\text{H}_4} K_{\text{trans-C}_4\text{H}_8, \text{LH}} P_{\text{trans-C}_4\text{H}_8} - \frac{1}{K_{\text{P, Met}}} K_{\text{C}_3\text{H}_6, \text{LH}}^2 P_{\text{C}_3\text{H}_6}^2}{1 + K_{\text{C}_2\text{H}_4, \text{LH}} P_{\text{C}_2\text{H}_4} + K_{\text{trans-C}_4\text{H}_8, \text{LH}} P_{\text{trans-C}_4\text{H}_8} + K_{\text{C}_3\text{H}_6, \text{LH}} P_{\text{C}_3\text{H}_6}^2} \quad (37)$$

#### Cracking (characteristic of network II)

$$r_{\text{Crack}}^{\text{LH}} = \frac{k_{\text{Crack}}^{\text{LH}} K_{\text{lump-C}_6, \text{LH}}^2 P_{\text{lump-C}_6}^2}{1 + K_{\text{lump-C}_6, \text{LH}} P_{\text{lump-C}_6} + K_{\text{C}_3\text{H}_6, \text{LH}} P_{\text{C}_3\text{H}_6}} \quad (38)$$

The temperature dependence of the adsorption equilibrium constants  $K_i^{\text{LHHW}}$  is typically less pronounced compared to the dependence of the corresponding reaction rate constants  $k_{\text{LH}}(T)$ . Thus, the former is often ignored, as done in the present work.

Furthermore, mono- and bimolecular adsorption processes are considered and summarized as LH. Isomerization and cracking are monomolecular kinetic approaches in which only one component has to adsorb onto the surface. In contrast, dimerization and metathesis are bimolecular processes in which two molecules necessarily have to adsorb. Nevertheless, in all reaction steps, each molecule can adsorb and, thus, block free surface sites.

## 5 Data Analysis and Parameter Estimation

### 5.1 Performance Parameters

The considered and detected eight components are ordered as follows: ethene, propene, ethane, the three butene isomers (1-, *cis*- and *trans*-butene), pentene and hexane ( $L_{\text{I}} = 7$  and  $L_{\text{II}} = 8$ ). *Iso*-butene was not considered, because it was not detected with sufficient confidence during the experiments carried out. Additionally, the isomers of pentene and hexene were lumped into pseudo-species  $\text{C}_5\text{H}_{10}$  and  $\text{C}_6\text{H}_{12}$ , because identification of the single isomers was not possible

with the analytical methods used. To evaluate the performance and to quantify the kinetics, the following performance criteria were used (Eqs. (39)–(41)).

*Conversion of ethene*

$$X_{C_2H_4} = \frac{\dot{n}_{C_2H_4}^0 - \dot{n}_{C_2H_4}^{ex}}{\dot{n}_{C_2H_4}^0} \quad (39)$$

*Selectivity of component i*

$$S_i = \frac{\dot{n}_i^{ex}}{\sum_{k=2}^{L_{Net}} \dot{n}_k} \quad i = 2, \dots, L_I = 7; L_{II} = 8 \quad (40)$$

*Yield of component i*

$$Y_i = \frac{\dot{n}_i^{ex}}{\dot{n}_{C_2H_4}^0} \frac{(-\nu_{C_2H_4})}{\nu_i} \quad i = 2, \dots, L_I = 7; L_{II} = 8 \quad (41)$$

The outlet molar fluxes were measured under steady-state conditions for a total number of 120 experimental runs ( $N_{ex} = 120$ ) for different operating conditions. Each experimental point was validated with three measurements. The deviations between the individual points of conversion, selectivity and yield were less than 5%. The extensive data set generated is used to estimate kinetic parameters, based on the two reaction networks described above, thereby quantifying the rates of  $j$  reactions characteristic for each of the two networks (see below).

## 5.2 Reactor Model and Parameter Estimation

To generate theoretical predictions corresponding to the experimental observations, the balance of a plug flow tubular reactor (PFTR) model (Eq. (42)) was solved numerically for all eight components involved in the reaction. The assumptions were that the system was at steady state for each experimental point and no backmixing was occurring. The catalyst bed was assumed to be isothermal and a pseudo-homogeneous model was implied for reduced complexity.

$$\frac{d\dot{n}_i}{dz} = \frac{m_{Cat}}{L} \sum_j \nu_{i,j} r_j(T, \bar{p}, \bar{P}_j) \quad i = 1, \dots, L_I = 7; L_{II} = 8 \quad (42)$$

The entity of performed experiments consisted of 120 experimental points ( $N_{ex} = 120$ ), with varying temperature, feed composition and  $W/F$ . Thus, each of the experiments ( $n = 1, \dots, Nex = 120$ ) generated up to 15 specific outputs ( $m = 1, \dots, M_{OUT,I} = 13$  and  $M_{OUT,II} = 15$ ), corresponding to the performance parameters conversion of the reactant ethene, the selectivity and yield of the seven intermediate products (propene, ethane, the three butene isomers, pentene and hexene), defined in Eqs. (39)–(41), indicated as  $Z_{m,n}^{ex}$ . Analysis of all reactions assumed ( $j$ ) dependent parameter vector  $\bar{P}_j$  was performed by minimizing the following objective function:

$$OF = \sum_n^{N_{ex}=120} \sum_m^{M_{Out,Net}} \left( Z_{m,n}^{ex} - Z_{m,n}^{th}(T, \bar{p}, \bar{P}_{j=1}, \dots, \bar{P}_{j=L}) \right)^2 \quad (43)$$

In the models, the temperature-dependent rate constants (part of the parameter vectors  $\bar{P}_j$ ) were described by Arrhenius expressions for the possible reactions:

$$k_j = k_{\infty,j} \exp\left(-\frac{E_{A,j}}{RT}\right) \quad (44)$$

To perform the calculation of Eqs. (39)–(41) for each reaction network, two solvers offered by Matlab 2016a (Version 9.0.0.341360) were used, namely “ODE15s” for solving Eq. (42) and “lsqnonlin” for minimizing  $OF$  (Eq. (43)) with the trust-region-reflective algorithm. This optimizer is based on the Levenberg-Marquardt algorithm. However, it approximates the objective function to a more straightforward function, with the estimated parameters being varied with a limited step size.

## 6 Analysis of the Kinetic Model for the Two Networks

An essential comprehensive parity plot is given in Fig. 2, which compares all modeling combinations considered in this work. The results obtained applying the LH model for network I are shown in the parity plot in Fig. 2a. It becomes clear that the measured data, particularly the ethene conversions, are represented well. An exception is an agreement regarding the selectivities of the desired product propene. The simulations significantly underestimate these values, with 0% selectivity, and attribute the converted ethene entirely to the dimerization and subsequent isomerization. This observation corresponds to the fact that the metathesis does not affect the product spectrum, which is not reasonable for network I. Thus, this network appears to be useful for the prediction of the dimerization and isomerization reaction products. An application of the LH modeling approach, using network I, presented accurate predictions of the butene isomers. Even though this proposed reaction network I is incapable of explaining the product spectrum, especially for propene, this appears to have minor implications on the simulative estimation. It is desirable to obtain better fitting for the two mentioned performance parameters for propene. Thus, this would make an application possible. It results in a less complicated system in need of less computational resources.

In comparison to the previous plot, LH model and network II (Fig. 2b) is capable of fitting all estimated conversions, selectivities and yields within a  $\pm 5\%$  margin compared to the experimental data. This is equivalent to the results of the LH model for the network I (Fig. 2a). However, the incorporation of cracking reactions can describe

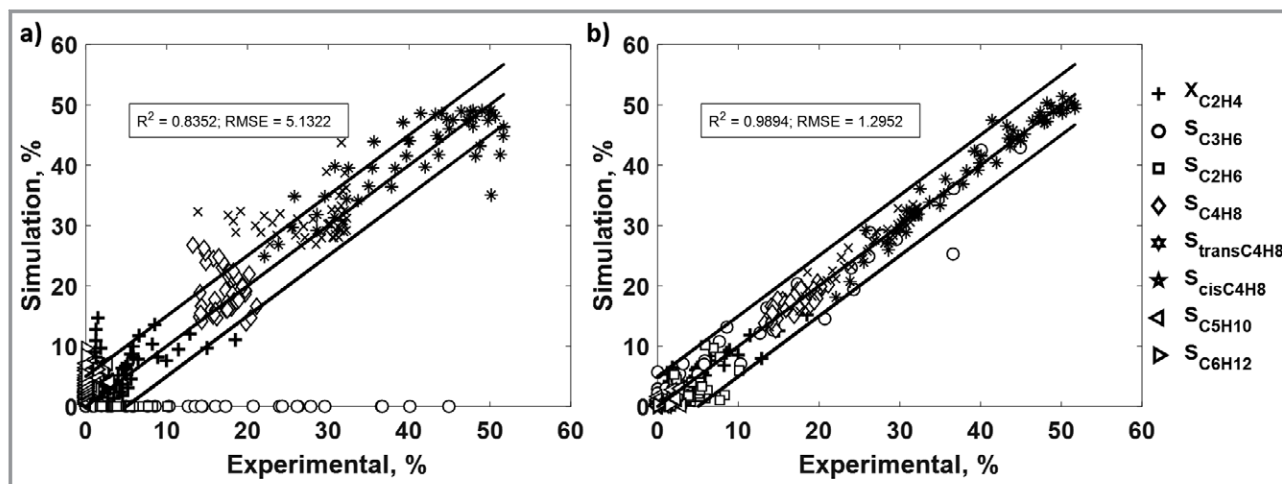


**Figure 2.** Comprehensive parity plots for applying the two evaluated reaction networks and the corresponding two types of modeling approaches. The basis for comparison is the reactor outlet data ( $z = L$ ) for a) network I applying LH equations ( $M_{OUT,I} = 13$ ) and  $Para_I = 39$  estimated parameters; b) modified network II using LH ( $M_{OUT,II} = 15$ ) and a number of estimated parameters  $Para_{II} = 54$ .

the conversion of ethene and the selectivity of propene adequately. The distribution of high selectivity values is limited, which implies better agreement and better applicability. The individual butene isomers, namely 1-, *cis*- and *trans*-butene, are entirely within the narrow error margin of  $\pm 5\%$ . Interestingly, the formerly underestimated desired products are now sufficiently matched, giving appropriate estimated values.

From the parity plots it can be concluded that the modified reaction network II is in better agreement and presents the following main results. The simulation results match well with experimentally observed molar outlet fluxes of all components analyzed. The production of all the analyzed products can be better explained.

Further analysis of network II, including network evaluation and parameter reduction, are presented in the following. Detailed information for network I using the LH model are provided in the Supporting Information (SI, Fig. S4). The results for network II implying catalytic cracking instead of metathesis will be discussed in more detail in the following section.

To illustrate typical trends, the results for the parametrized rate expressions applying the LH model for the modified network II are presented. In the optimization process, the objective function Eq. (43) was minimized. As discussed above, this combination provided the most satisfying results. The estimated model parameters of the 24 equations formulated in network II and the LH approach are summarized in Tab. S1. Experimentally determined and simulated conversion and selectivity data are shown in Fig. 3.

In Fig. 3a, the quality of the agreement can be seen for the conversion of ethene. The initial activity at 200 °C does not fit accurately for higher feed concentrations. Nevertheless, the model represents the essential features of the ethene conversion trends for varying reaction conditions. More details regarding the quality of describing the ethene

conversion with this model are shown for varying  $W/F$  in Fig. S2, as well as the concentration in Figs. S1 and S3. The calculated simulative results represent the concentration profiles well. In contrast, the trend in conversion is not sufficiently represented for varying  $W/F$  ratios. Here the slopes are not matched, and local extrema are not well included by the model. The limited quality of the ethene conversion predictions indicates the limits in the reactor model. This can be explained by the fact that the catalyst bed is more inhomogeneous than assumed for the reactor model. Further, channeling or diffusive effects could decline the accuracy. Nevertheless, the results are in good agreement and with this estimation, a more complex model can be investigated in further research.

The model predictions are much better regarding propene selectivity (Fig. 3b). The selectivity begins to increase at a temperature of approx. 250 °C. At higher temperatures, the predictions follow the observed trends in a wide range of reaction conditions. However, not all individual reaction conditions can be separated. As a result, the fit is not entirely accurate. That is why the propene selectivity in Fig. 2b shows minimal differences between simulation and experiment for high values.

The butene isomers are crucial for comparing network I and II since they are considered differently. Their selectivities are predicted quite well, assuming network II and the LH modeling approach for the entire reaction conditions and the temperature range. For 1-butene (Fig. 3c), in agreement with the observed experimental results, the model is capable of predicting an increase until an inflection point is reached around 275 °C. The influence of feed concentration is also well described. A reasonable agreement between measurements and prediction is also observed for *trans*-butene, as shown in Fig. 3d.

As already shown in the parity plots, the use of the modified reaction network II results in a more consistent

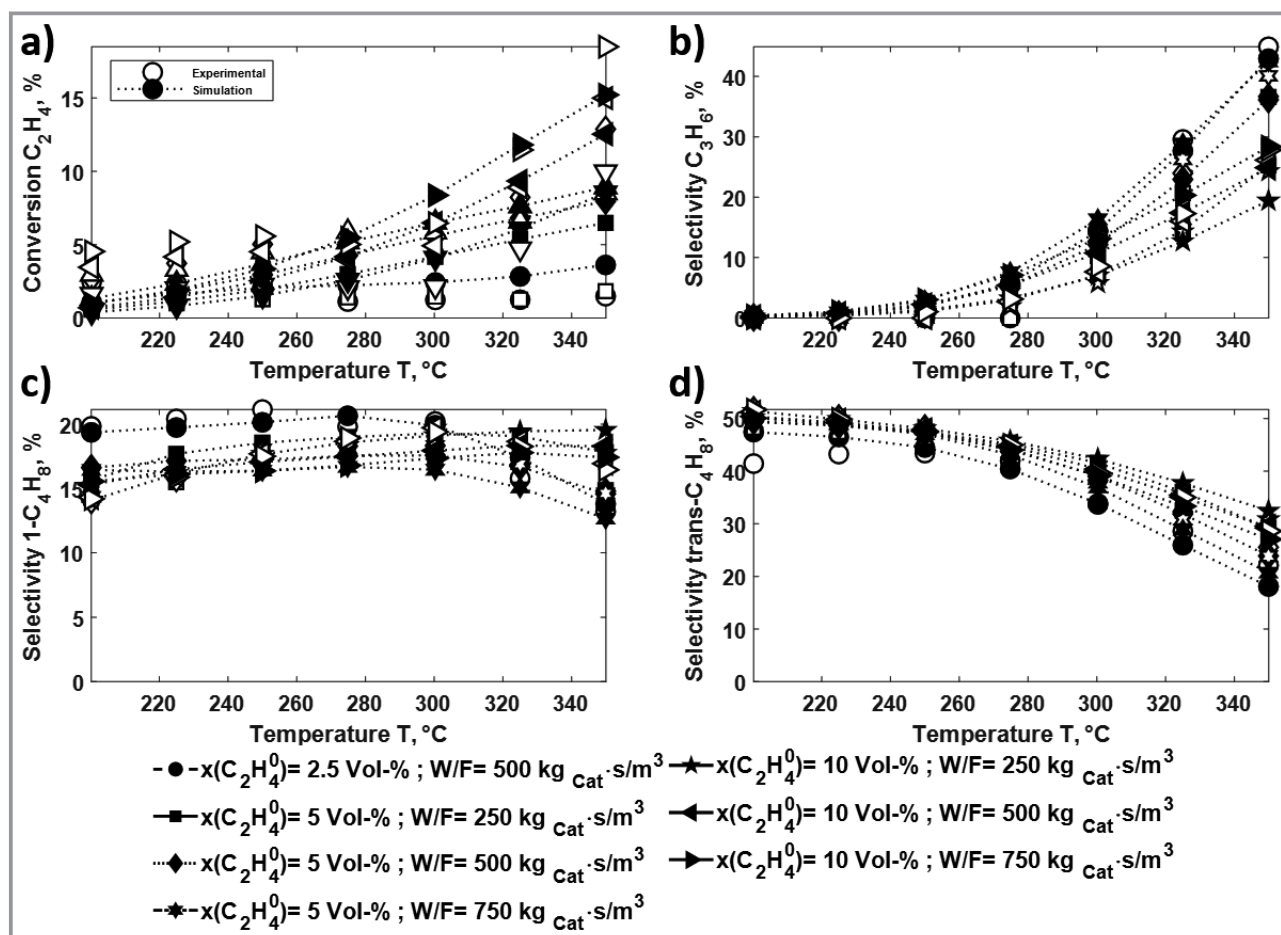


**Figure 3.** The effect of temperature for varying feed concentrations and  $W/F$  ratios applying the LH approach in combination with the modified reaction network II. a) Conversion of ethene; b) propene selectivity; c) 1-butene selectivity; d) trans-butene selectivity and  $Para_{II} = 56$  estimated parameters, with reaction conditions of ethene feed and  $W/F$ , for  $J_{II} = 24$  reaction considered and  $M_{OUT,II} = 15$  performance parameter.

agreement of the simulative results with the experimental observations. Thus, the outputs are sufficiently well represented, in contrast to network I, which integrates the metathesis reaction. With the help of the modified network II, including cracking and a larger number of reactions with  $J_{II} = 24$ , the resulting parametrized equations appear more suitable for the applied catalytic system. For the main products, the order of the different experimental conditions, as well as the trends and inflection points, are displayed excellently. Even if the network is more complex, an appealing result is achieved with the assumption of a cracking reaction network. Further attempts to reduce the complexity of the network were undertaken, but not reported here. A summary is given in the Supporting Information.

## 7 Conclusions

The heterogeneously catalyzed direct synthesis of propene from ethene was studied on a Ni/AlMCM-41 catalyst with a Si/Al ratio of 60. Two different reaction networks and their

catalytic cycles were evaluated and compared. At first, the established reaction network I suggested by Iwamoto [3], consisting of dimerization, isomerization and metathesis steps, was considered. During validation, this network presented no selectivity towards the desired product propene, contrary to the experimental results. In an attempt to improve the representation of the experimental data, a modified reaction network II was assumed, based on the observation and in accordance to literature. In this network, catalytic cracking was considered rather than a metathesis step. The application of this approach improved the agreement of the experiments with the predicted values. Better quantification of the observed product spectra is possible. This modified reaction network II is still limited to quantify components up to  $C_6$  (hexene).

The application of the Langmuir-Hinshelwood-Hougen-Watson (LH) for parametrizing the equations of the network including the catalytic cracking mechanism, resulted in a satisfactory representation of the experimentally obtained data. For the set of 24 reactions, kinetic parameters were estimated.



In future work, the kinetic model derived for network II will be used in combination with a required extension for the additional description of both the deactivation and the regeneration of the catalytic system. Based on this, cyclic process conditions will be derived.

## Supporting Information

Supporting Information for this article can be found under DOI: <https://doi.org/10.1002/cite.201900139>.

We want to acknowledge and thank the DAAD (Germany) and CONACYT (Mexico) for their funding of the international exchange of knowledge. Funding by the Deutsche Forschungsgemeinschaft (DFG, German Research Foundation) – TRR 63 “Integrated Chemical Processes in Liquid Multiphase Systems” (subprojects A3) – 56091768 is gratefully acknowledged. Further, we would like to thank Jutta Wilke for supporting the experimental realization and the colleagues at the OvGU for helpful discussions.

## Symbols used

$E_A$	[kJ mol <sup>-1</sup> ]	activation energy
$J$	[-]	total number of reactions involved in each reaction network
$k$	[variable]	reaction rate constant
$k_\infty$	[variable]	collision factor
$K_i$	[Pa <sup>-1</sup> ]	equilibrium constant of adsorption of component $i$
$L$	[-]	total number of involved components
$m$	[-]	number of performance parameter
$M_{Out}$	[-]	total number of performance parameters used
$n$	[-]	experimental number
$\dot{n}$	[mol s <sup>-1</sup> ]	molar flow
$N_{ex}$	[-]	total number of experiments performed
$p$	[Pa]	pressure
$Par$	[-]	number of parameters for each reaction network
$r$	[mol kg <sub>Cat</sub> s <sup>-1</sup> ]	reaction rate
$R$	[J mol <sup>-1</sup> K <sup>-1</sup> ]	universal gas constant
$S$	[%]	selectivity
$T$	[K]	temperature
$W/F$	[kg <sub>Cat</sub> s m <sup>-3</sup> ]	weight to flow
$X$	[%]	conversion
$Y$	[%]	yield

## Greek letters

$\nu_i$	[-]	stoichiometric coefficient of component $i$
$\lambda_i$	[-]	frequency function for mechanistic modeling

## Sub- and Superscripts

Cat	catalyst
Crack	cracking reaction
Dim	dimerization reaction
ex	experimental value
$i$	specific component
Iso	isomerization reaction
$j$	specific reaction
$k$	product component
LH	Langmuir-Hinshelwood-Hougen-Watson
Lump-C <sub>6</sub>	lumped hexane species
Met	Langmuir-Hinshelwood-Hougen-Watson
Net	indication of the used network I or II'
Prod	product
Reac	reactant
th	theoretical value
0	initial value indication

## Abbreviations


CP-MAS	cross polarization magic-angle spinning
ETP	ethene to propene
HTKR	high-temperature kinetic reactor
LH	Langmuir-Hinshelwood-Hougen-Watson
MCM	Mobil Composition of Matter
MM	mechanistic modeling
PFTR	plug flow tubular reactor
SAPO	small-pore molecular sieves
ZSM	Zeolite Socony Mobil

## References


- [1] A. V. Lavrenov, L. F. Saifulina, E. A. Buluchevskii, E. N. Bogdanets, *Catal. Ind.* **2015**, *7* (3), 175–187. DOI: <https://doi.org/10.1134/S2070050415030083>
- [2] L. Alvarado Perea, T. Wolff, P. Veit, L. Hilfert, F. T. Edelmann, C. Hamel, A. Seidel-Morgenstern, *J. Catal.* **2013**, *305*, 154–168. DOI: <https://doi.org/10.1016/j.jcat.2013.05.007>
- [3] M. Iwamoto, *Catal. Surv. Asia* **2008**, *12* (1), 28–37. DOI: <https://doi.org/10.1007/s10563-007-9036-y>
- [4] M. Taoufik, E. Le Roux, J. Thivolle-Cazat, J.-M. Basset, *Angew. Chem., Int. Ed.* **2007**, *46* (38), 7202–7205. DOI: <https://doi.org/10.1002/anie.200701199>
- [5] H. Oikawa, Y. Shibata, K. Inazu, Y. Iwase, K. Murai, S. Hyodo, G. Kobayashi, T. Baba, *Appl. Catal., A* **2006**, *312*, 181–185. DOI: <https://doi.org/10.1016/j.apcata.2006.06.045>


- [6] B. Lin, Q. Zhang, Y. Wang, *Ind. Eng. Chem. Res.* **2009**, *48* (24), 10788–10795. DOI: <https://doi.org/10.1021/ie901227p>
- [7] M. Iwamoto, *Molecules (Basel, Switzerland)* **2011**, *16* (9), 7844–7863. DOI: <https://doi.org/10.3390/molecules16097844>
- [8] T. Lehmann, T. Wolff, C. Hamel, P. Veit, B. Garke, A. Seidel-Morgenstern, *Microporous Mesoporous Mater.* **2012**, *151*, 113–125. DOI: <https://doi.org/10.1016/j.micromeso.2011.11.006>
- [9] T. Lehmann, T. Wolff, V. M. Zahn, P. Veit, C. Hamel, A. Seidel-Morgenstern, *Catal. Commun.* **2011**, *12* (5), 368–374. DOI: <https://doi.org/10.1016/j.catcom.2010.10.018>
- [10] L. Alvarado Perea, *Direct conversion of ethene to propene on Ni-alumino-mesostructured catalysts: synthesis, characterization and catalytic testing*, Dissertation, Otto-von-Guericke Universität, Magdeburg **2014**.
- [11] L. Alvarado Perea, T. Wolff, C. Hamel, A. Seidel-Morgenstern, *Appl. Catal., A* **2017**, *533*, 121–131. DOI: <https://doi.org/10.1016/j.apcata.2016.12.022>
- [12] P. Pérez-Urriarte, A. Ateka, A. T. Aguayo, A. G. Gayubo, J. Bilbao, *Chem. Eng. J.* **2016**, *302*, 801–810. DOI: <https://doi.org/10.1016/j.cej.2016.05.096>
- [13] H. C. Beirnaert, J. R. Alleman, G. B. Marin, *Ind. Eng. Chem. Res.* **2001**, *40* (5), 1337–1347. DOI: <https://doi.org/10.1021/ie0004971>
- [14] T. von Aretin, O. Hinrichsen, *Ind. Eng. Chem. Res.* **2014**, *53* (50), 19460–19470. DOI: <https://doi.org/10.1021/ie503628p>
- [15] E. Epelde, A. T. Aguayo, M. Olazar, J. Bilbao, A. G. Gayubo, *Ind. Eng. Chem. Res.* **2014**, *53* (26), 10599–10607. DOI: <https://doi.org/10.1021/ie501533j>
- [16] A. G. Gayubo, A. Alonso, B. Valle, A. T. Aguayo, J. Bilbao, *Ind. Eng. Chem. Res.* **2010**, *49* (21), 10836–10844. DOI: <https://doi.org/10.1021/ie100407d>
- [17] S. H. Mousavi, S. Fatemi, M. Razavian, *Reac. Kinet., Mech. Catal.* **2017**, *122* (2), 1245–1264. DOI: <https://doi.org/10.1007/s11144-017-1266-z>
- [18] H. Zhou, Y. Wang, F. Wei, D. Wang, Z. Wang, *Appl. Catal., A* **2008**, *348* (1), 135–141. DOI: <https://doi.org/10.1016/j.apcata.2008.06.033>
- [19] V. Van Speybroeck, K. de Wispelaere, J. Van der Mynsbrugge, M. Vandichel, K. Hemelsoet, M. Waroquier, *Chem. Soc. Rev.* **2014**, *43* (21), 7326–7357. DOI: <https://doi.org/10.1039/c4cs00146j>
- [20] R. R. Pinto, P. Borges, M. A. N. D. A. Lemos, F. Lemos, F. Ramôa Ribeiro, *Appl. Catal., A* **2004**, *272* (1–2), 23–28. DOI: <https://doi.org/10.1016/j.apcata.2004.02.004>
- [21] S. Lwin, I. E. Wachs, *ACS Catal.* **2016**, *6* (1), 272–278. DOI: <https://doi.org/10.1021/acscatal.5b02233>
- [22] F. Kapteijn, H. L. G. Bredt, E. Homburg, J. C. Mol, *Ind. Eng. Chem. Prod. Res. Dev.* **1981**, *20*, 457–466.
- [23] E. A. Buluchevskiy, A. V. Lavrenov, L. F. Sayfulina, *J. Sib. Fed. Univ.* **2014**, *3* (7), 424–430.
- [24] M. Felischak, T. Wolff, L. Alvarado Perea, A. Seidel-Morgenstern, C. Hamel, *Chem. Eng. Sci.* **2019**, *210*, 115246. DOI: <https://doi.org/10.1016/j.ces.2019.115246>
- [25] H. A. Wittcoff, B. G. Reuben, J. S. Plotkin, *Industrial organic chemicals*, 3rd ed., Wiley, Hoboken, NJ **2013**.
- [26] X. Zhu, S. Liu, Y. Song, S. Xie, L. Xu, *Appl. Catal., A* **2005**, *290* (1–2), 191–199. DOI: <https://doi.org/10.1016/j.apcata.2005.05.028>
- [27] X. Zhu, S. Liu, Y. Song, L. Xu, *Appl. Catal., A* **2005**, *288* (1–2), 134–142. DOI: <https://doi.org/10.1016/j.apcata.2005.04.050>
- [28] B. Wang, Q. Gao, J. Gao, D. Ji, X. Wang, J. Suo, *Appl. Catal., A* **2004**, *274* (1–2), 167–172. DOI: <https://doi.org/10.1016/j.apcata.2004.06.037>
- [29] X. Zhu, S. Liu, Y. Song, L. Xu, *Catal Lett* **2005**, *103* (3–4), 201–210. DOI: <https://doi.org/10.1007/s10562-005-7155-5>
- [30] J. Lu, Z. Zhao, C. Xu, A. Duan, P. Zhang, *Catal. Lett.* **2006**, *109* (1–2), 65–70. DOI: <https://doi.org/10.1007/s10562-006-0058-2>
- [31] J. S. Buchanan, J. G. Santiesteban, W. O. Haag, *J. Catal.* **1996**, *158*, 279–287.
- [32] A. Corma, A. V. Orchillés, *Microporous Mesoporous Mater.* **2000**, *35–36*, 21–30. DOI: [https://doi.org/10.1016/S1387-1811\(99\)00205-X](https://doi.org/10.1016/S1387-1811(99)00205-X)
- [33] P. J.-L. Herisson, Y. Chauvin, *Makromol. Chem.* **1971**, *141* (1), 161–176.
- [34] R. H. Grubbs, *Tetrahedron* **2004**, *60* (34), 7117–7140. DOI: <https://doi.org/10.1016/j.tet.2004.05.124>
- [35] R. D. Andrei, M. I. Popa, C. Cammarano, V. Hulea, *New J. Chem.* **2016**, *40* (5), 4146–4152. DOI: <https://doi.org/10.1039/C5NJ02586A>
- [36] K. J. Laidler, J. H. Meiser, *Physical chemistry*, Benjamin-Cummings Publishing Company, Menlo Park, CA **1982**.
- [37] I. Langmuir, *J. Am. Chem. Soc.* **1916**, *38* (11), 2221–2295.
- [38] F. G. Helfferich, *Kinetics of multistep reactions*, 2nd ed., Comprehensive chemical kinetics, v. 40, Elsevier, Amsterdam **2004**.
- [39] D. Murzin, T. Salmi, *Catalytic Kinetics*, Elsevier, Amsterdam **2005**.
- [40] G. Kiedorf, D. M. Hoang, A. Müller, A. Jörke, J. Markert, H. Arellano-Garcia, A. Seidel-Morgenstern, C. Hamel, *Chem. Eng. Sci.* **2014**, *115*, 31–48. DOI: <https://doi.org/10.1016/j.ces.2013.06.027>
- [41] I. Mueller, G. Kiedorf, E. Runne, I. Pottratz, A. Seidel-Morgenstern, C. Hamel, *Chem. Ing. Tech.* **2018**, *90* (5), 725–730. DOI: <https://doi.org/10.1002/cite.201700152>
- [42] S. M. Alwahabi, G. F. Froment, *Ind. Eng. Chem. Res.* **2004**, *43* (17), 5098–5111. DOI: <https://doi.org/10.1021/ie040041u>
- [43] K. Norinaga, O. Deutschmann, *Ind. Eng. Chem. Res.* **2007**, *46* (11), 3547–3557. DOI: <https://doi.org/10.1021/ie061207p>
- [44] K. Norinaga, O. Deutschmann, N. Saegusa, J.-i. Hayashi, *J. Anal. Appl. Pyrolysis* **2009**, *86* (1), 148–160. DOI: <https://doi.org/10.1016/j.jaap.2009.05.001>
- [45] K. Norinaga, V. M. Janardhanan, O. Deutschmann, *Int. J. Chem. Kinet.* **2008**, *40* (4), 199–208. DOI: <https://doi.org/10.1002/kin.20302>
- [46] K. Amakawa, S. Wrabetz, J. Kröhnert, G. Tzolova-Müller, R. Schlögl, A. Trunschke, *J. Am. Chem. Soc.* **2012**, *134* (28), 11462–11473. DOI: <https://doi.org/10.1021/ja3011989>
- [47] M. Argyle, C. Bartholomew, *Catalysts* **2015**, *5* (1), 145–269. DOI: <https://doi.org/10.3390/catal5010145>
- [48] M. Hartmann, A. Pöpl, L. Kevan, *J. Phys. Chem. C* **1996**, *100*, 9906–9910.
- [49] L. Bonneviot, D. Olivier, M. Che, *J. Mol. Catal. A: Chem.* **1983**, *21*, 415–430.
- [50] R. D. Broene, M. Brookhart, W. M. Lamanna, A. F. Volpe, *J. Am. Chem. Soc.* **2005**, *127* (49), 17194–17195. DOI: <https://doi.org/10.1021/ja056655n>
- [51] J. R. Sohn, W. C. Park, *Korean J. Chem. Eng.* **2000**, *17* (6), 727–730.
- [52] J. R. Sohn, W. C. Park, D. C. Shin, *J. Mol. Catal. A: Chem.* **2006**, *256* (1–2), 156–163. DOI: <https://doi.org/10.1016/j.molcata.2006.04.069>
- [53] R. D. Andrei, M. I. Popa, F. Fajula, V. Hulea, *J. Catal.* **2015**, *323*, 76–84. DOI: <https://doi.org/10.1016/j.jcat.2014.12.027>
- [54] J. Rabeah, J. Radnik, V. Briois, D. Maschmeyer, G. Stochniol, S. Peitz, H. Reeker, C. La Fontaine, A. Brückner, *ACS Catal.* **2016**, *6* (12), 8224–8228. DOI: <https://doi.org/10.1021/acscatal.6b02331>
- [55] M. J. Baird, J. H. Lunsford, *J. Catal.* **1972**, *26*, 440–450.
- [56] P. Dejaviève, *J. Catal.* **1980**, *63* (2), 331–345. DOI: [https://doi.org/10.1016/0021-9517\(80\)90086-X](https://doi.org/10.1016/0021-9517(80)90086-X)

- [57] O. Bortnovsky, P. Sazama, B. Wichterlova, *Appl. Catal., A* **2005**, 287 (2), 203–213. DOI: <https://doi.org/10.1016/j.apcata.2005.03.037>
- [58] C.-J. Chen, S. Rangarajan, I. M. Hill, A. Bhan, *ACS Catal.* **2014**, 4 (7), 2319–2327. DOI: <https://doi.org/10.1021/cs500119n>
- [59] X. Huang, D. Aihemaitijiang, W.-D. Xiao, *Chem. Eng. J.* **2015**, 280, 222–232. DOI: <https://doi.org/10.1016/j.cej.2015.05.124>
- [60] E. Epelde, A. T. Aguayo, M. Olazar, J. Bilbao, A. G. Gayubo, *Appl. Catal., A* **2014**, 479, 17–25. DOI: <https://doi.org/10.1016/j.apcata.2014.04.005>
- [61] G. F. Froment, *Rev. Chem. Eng.* **2013**, 29 (6), 385–412. DOI: <https://doi.org/10.1515/revce-2013-0019>
- [62] P. M. Slomkiewicz, *Appl. Catal., A* **2004**, 269 (1–2), 33–42. DOI: <https://doi.org/10.1016/j.apcata.2004.03.055>
- [63] W. O. Haag, H. Pines, *J. Am. Chem. Soc.* **1960**, 82, 2488–2494.
- [64] C.-M. Wang, Y.-D. Wang, J. Dong, S. Liu, Z.-K. Xie, *Comput. Theor. Chem.* **2011**, 974 (1–3), 52–56. DOI: <https://doi.org/10.1016/j.comptc.2011.07.011>
- [65] R. Cramer, *J. Am. Chem. Soc.* **1966**, 88 (10), 2272–2282. DOI: <https://doi.org/10.1021/ja00962a034>




**Neugierig?**






**Erlebnis Wissenschaft**



**NEU**



**NEU**


**GERD GANTEFÖR**  
**Wir drehen am Klima**  
– na und?  
*ISBN: 978-3-527-33778-1*  
*September 2015 238 S. mit 50 Abb.*  
*Gebunden € 24,90*

Das neue Buch von Gerd Ganteför provoziert: Ohne Klimakontrolle durch den Menschen können wir den Klimawandel nicht beherrschen!  
Gerd Ganteför vertritt in seinem Buch zwei starke und umstrittene Thesen. Erstens: Die Energiewende als Mittel gegen die Klimaerwärmung versagt. Zweitens: Wir brauchen einen Plan B, die aktive, zielgerichtete Klimakontrolle.  
Provokant, meinungsstark, einzigartig – das erste Buch, das eine aktive Klimakontrolle propagiert!

**LEOPOLD MATHELITSCHE und SIGRID THALLER**  
**Physik des Sports**  
*ISBN: 978-3-527-41304-1*  
*September 2015 168 S. mit 100 Abb.*  
*Gebunden € 24,90*

Kenntnisse aus Physik und Sport haben zwar auf den ersten Blick nicht viel gemeinsam, sind aber bei genauerer Betrachtung untrennbar. Für das Verständnis von sportlichen Bewegungen braucht man Wissen aus der Physik!  
In diesem Buch werden die physikalischen Gesetzmäßigkeiten offenbart, die über Erfolg oder Misserfolg entscheiden.  
Folgende Sportarten werden behandelt: Fußball, Tennis, Golf, Volleyball, Baseball, Geräteturnen, Schwimmen, Tauchen, Skifahren, Skispringen, Eishockey, Kampfsport und Reiten.

[www.wiley-vch.de/sachbuch](http://www.wiley-vch.de/sachbuch)



Auch als  
E-Books unter:  
[www.wiley-vch.de/ebooks/](http://www.wiley-vch.de/ebooks/)

**WILEY-VCH**

Irrtum und Preisänderungen vorbehalten. Stand der Daten: August 2015.

Wiley-VCH • Postfach 10 11 61 • D-69451 Weinheim  
Tel. +49 (0)6201-606400 • e-mail: [service@wiley-vch.de](mailto:service@wiley-vch.de)